RESEARCH ARTICLE • OPEN ACCESS

A Discrete Predator-Prey Model with Cannibalism, Refuge, and Memory Effect: Implementation of Piecewise Constant Argument (PWCA) Method

Maya Rayungsari *et al.*

Volume 6, Issue 1, Pages 23–34, March 2025

Received 28 December 2024, Revised 22 February 2025, Accepted 27 March 2025, Published Online 31 March 2025

To Cite this Article : M. Rayungsari *et al.*,"A Discrete Predator-Prey Model with Cannibalism, Refuge, and Memory Effect: Implementation of Piecewise Constant Argument (PWCA) Method", *Jambura J. Biomath*, vol. 6, no. 1, pp. 23–34, 2025, *https://doi.org/10.37905/jjbm.v6i1.29391*

JOURNAL INFO • JAMBURA JOURNAL OF BIOMATHEMATICS

Homepage	:	http://ejurnal.ung.ac.id/index.php/JJBM/index
Journal Abbreviation	:	Jambura J. Biomath.
Frequency	:	Biannual (June and December)
Publication Language	:	English
DOI	:	https://doi.org/10.37905/jjbm
Online ISSN	:	2723-0317
Editor-in-Chief	:	Hasan S. Panigoro
Publisher	:	Department of Mathematics, Universitas Negeri Gorontalo
Country	:	Indonesia
OAI Address	:	http://ejurnal.ung.ac.id/index.php/jjbm/oai
Google Scholar ID	:	XzYgeKQAAAAJ
Email	:	editorial.jjbm@ung.ac.id

JAMBURA JOURNAL • FIND OUR OTHER JOURNALS

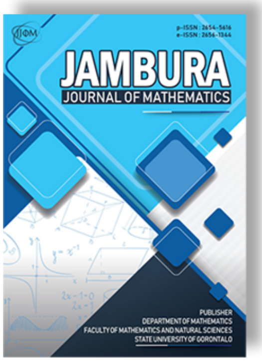

Jambura Journal of Mathematics

Jambura Journal of Mathematics Education

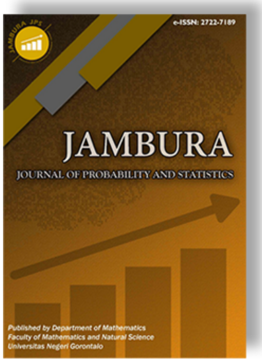

Jambura Journal of Probability and Statistics

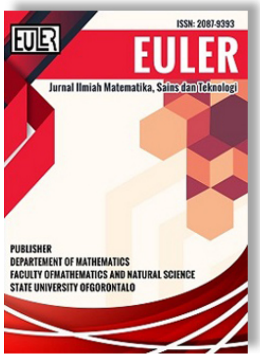

EULER : Jurnal Ilmiah Matematika, Sains, dan Teknologi

Jambura Journal of Biomathematics, Volume 6, Issue 1, Pages 23–34, March 2025 https://doi.org/10.37905/jjbm.v6i1.29391

Research Article

Check for updates

A Discrete Predator-Prey Model with Cannibalism, Refuge, and Memory Effect: Implementation of Piecewise Constant Argument (PWCA) Method

Maya Rayungsari[1,*], **Dewi Nurmalitasari**[2], and **Edy Tya Gullit Duta Pamungkas**[3]

[1]*Computer Science Study Program, Universitas PGRI Wiranegara, Pasuruan 67118, Indonesia*
[2]*Mathematics Education Study Program, Universitas PGRI Wiranegara, Pasuruan 67118, Indonesia*
[3]*Food Technology Study Program, Universitas PGRI Wiranegara, Pasuruan 67118, Indonesia*

ARTICLE HISTORY
Received 28 December 2024
Revised 22 February 2025
Accepted 27 March 2025
Published 31 March 2025

KEYWORDS
Discrete dynamics
Predator-prey model
Piecewise Constant Argument (PWCA)
Cannibalism and refuge
Memory effect

ABSTRACT. *Predator-prey models are essential for understanding ecological dynamics, and fractional-order models provide a more realistic approach by considering memory effects. This study aims to analyze the discrete dynamics of a predator-prey model, incorporating predator cannibalism, refuge, and memory effects with a Caputo-type fractional-order. The Piecewise Constant Argument (PWCA) method was employed for discretization, followed by an analysis of the equilibrium points and their stability. Four equilibrium points were identified: the origin, prey extinction, predator extinction, and coexistence. It was found that the origin point was unstable, while the prey extinction, predator extinction, and coexistence points were conditionally locally asymptotically stable, depending on the parameter values. The order of the fractional derivative and step size significantly influenced the stability of these equilibrium points. Numerical simulations confirmed the theoretical findings, showing how parameter variations affect system behavior.*

1. Introduction

Interactions between predators and their prey are critical to balancing ecosystems [1]. These interactions keep the population in check, prevent species from overpopulating the environment. Predators regulate prey populations to prevent resource overconsumption, while prey species ensure a constant food reservoir conducive to predator survival [2]. One of the best documented system in this regard is the relationship between the brown planthopper (*Nilaparvata lugens*) and the wolf spider (Lycosidae). The brown planthopper is among the most damaging of rice pests and severely reduces yields in many Asian countries, e.g. Indonesia [3, 4]. Alternatively, the wolf spider is a natural enemy that can regulate the population of planthopper through predation [5, 6].

The simple predator-prey relationship is more complex in this system owing to a number of ecological processes such a cannibalism between predators [7–9] and refuge strategies [10–12]. Predator cannibalism, as shown in wolf spiders, can greatly affect population dynamics [13]. Wolf spiders can sometimes resort to cannibalising other individuals of the same species, particularly when food sources are less abundant or in some developmental stages [14]. Wolf spiders, on the other hand, use refuge strategies for both intraspecific predation (cannibalism) and external threats.

Mathematical models including the predator cannibalism and refuge have been previously addressed in multiple studies [15–17]. Most predator-prey system dynamics are observed using integer-order models, but one of the new approaches is the use of fractional-order models [18–20]. The fractional-order models can capture memory effects and the influence of all previous states oh the dynamics. In ecological systems, it is common for past interactions—predator-prey interactions, environmental changes, or population densities—have an impact on the current dynamics. These systems use memory effects, where the current state is not only affected by prevailing conditions but also by historical trends.

Fractional derivatives, particularly the Caputo derivative, allows for a memory effect into the mathematical model [21, 22]. While classical derivatives center solely on the current rate of change, Caputo derivative accommodate the effect from historical states [23]. Fractional-order can thus be an excellent choice for biological systems where processes such as reproduction, migration, and predation take time to have effect [24]. This approach also provides a useful way of modeling scenarios in which population responses to environmental changes are not instantaneous, but instead build up over time.

Fractional-order models modified by the Caputo derivative have become common tool for describing ecological systems more accurately. Additionally, discrete approaches utilizing the Piecewise Constant Argument (PWCA) method are increasingly employed to represent population phenomena that change discretely, particularly in environments with high temporal variability [20]. A more realistic framework for populations where changes happen at discrete time increments rather than contin-

*Corresponding Author.

Email : *maya.rayungsari@gmail.com* (M. Rayungsari)
Homepage : http://ejurnal.ung.ac.id/index.php/JJBM/index / E-ISSN : 2723-0317

ually. Additionally, discrete-time models enable more effective computational results for numerical calculations and exhibit interesting dynamics with regard to continuous systems. [25, 26]. This strategy is particularly beneficial in ecological studies where population data are obtained at distinct time periods, such as seasonal or annual population surveys. Compared to other discretization techniques, the PWCA method offers the advantage of being able to readily conduct stability analysis, even in situations where the system contains fractional-order derivatives. The use of the PWCA method to solve fractional-order systems was proposed by [27]. However, this method has rarely been used in the dynamic analysis of fractional-order predator-prey models [20, 28, 29]. Therefore, this study contributes to expanding the reference on the dynamic analysis of predator-prey models involving memory effects, using fractional-order derivatives of the Caputo type and the PWCA discretization method.

Table 1. Description of parameters

Parameter	Description
r	Intrinsic growth rate of prey
K	Carrying capacity of prey
a_1	Maximum prey predation rate by predator
b_1	Half saturation constant of prey predation by predator
c_1	Conversion rate of prey predation into predator biomass
a_2	Maximum predator cannibalism rate
b_2	Half saturation constant of predator cannibalism
c_2	Conversion rate of cannibalism into predator biomass
m	Natural mortality rate of predator
p	Proportion of predator cannibalism

The prior study, [15], proposed a predator-prey model with cannibalism and predator refuge,

$$\begin{aligned} \frac{dX}{dt} &= rX\left(1-\frac{X}{K}\right)-\frac{a_1XY}{b_1+X}, \\ \frac{dY}{dt} &= \frac{c_1XY}{b_1+X}+c_2Y-mY-\frac{a_2(1-p)Y^2}{b_2+(1-p)Y}, \end{aligned} \tag{1}$$

with X and Y are prey and predator density, respectively. The parameters of system (1) are positive constant described in Table 1. System (1) was motified by [30]. [16] further extended the model by incorporating memory effects through the fractional-order Caputo derivative,

$$\begin{aligned} D_*^{\alpha}X &= rX\left(1-\frac{X}{K}\right)-\frac{a_1XY}{b_1+X}, \\ D_*^{\alpha}Y &= \frac{c_1XY}{b_1+X}+c_2Y-mY-\frac{a_2(1-p)Y^2}{b_2+(1-p)Y}, \end{aligned} \tag{2}$$

with $\alpha \in \mathbb{R}$, $0 < \alpha \leq 1$, and D_*^{α} is the Caputo fractional derivative operator defined as

$$D_*^{\alpha}x(t) = I^{1-\alpha}x'(t), t \geq 0. \tag{3}$$

$I^{1-\alpha}$ in eq. (3) represents the Riemann-Liouville fractional integral, which is defined by

$$I^{1-\alpha}x(t) = \frac{1}{\Gamma(1-\alpha)}\int_0^t (t-s)^{-\alpha}x(s)\,ds. \tag{4}$$

In this study, we implement a discrete method using PWCA to modify system (2). This modification allows us to examine how discrete-time dynamics influence predator-prey stability when memory effects, refuge, and cannibalism are considered together.

This study investigates not only the numerical implementation of the PWCA method but also the ecological implications of integrating discrete-time memory effects, predator refuge, and cannibalism. The goal of the modeling is to assess how these factors impact population stability within a discrete system. The paper is structured as follows: Section 2 details the model discretization using the PWCA method. The results of the dynamic analysis, including the existence and stability of equilibrium points, are presented in Section 3. Section 5 provides a summary of the main findings of the study, while Section 4 provides numerical simulations to validate the analytical findings.

2. Model formulation

In this section, we employ the Piecewise Constant Argument (PWCA) scheme to derive the discrete form of the model (2). We followed a similar approach used in a previous study [28] to discretize eq. (2).

$$\begin{aligned} D_*^{\alpha}X &= rX\left(\left[\frac{\tau}{h}\right]h\right)\left(1-\frac{X\left(\left[\frac{\tau}{h}\right]h\right)}{K}\right) \\ &\quad -\frac{a_1X\left(\left[\frac{\tau}{h}\right]h\right)Y\left(\left[\frac{\tau}{h}\right]h\right)}{b_1+X\left(\left[\frac{\tau}{h}\right]h\right)}, \\ D_*^{\alpha}Y &= \frac{c_1X\left(\left[\frac{\tau}{h}\right]h\right)Y\left(\left[\frac{\tau}{h}\right]h\right)}{b_1+X\left(\left[\frac{\tau}{h}\right]h\right)}+c_2Y\left(\left[\frac{\tau}{h}\right]h\right) \\ &\quad -mY\left(\left[\frac{\tau}{h}\right]h\right)-\frac{a_2(1-p)Y^2\left(\left[\frac{\tau}{h}\right]h\right)}{b_2+(1-p)Y\left(\left[\frac{\tau}{h}\right]h\right)}, \end{aligned} \tag{5}$$

with initial conditions $X(0) = X_0$ and $Y(0) = Y_0$. For $\tau \in [0,h)$, $\frac{\tau}{h} \in [0,1)$, and according to eq. (5), we get

$$\begin{aligned} D_*^{\alpha}X &= rX_0\left(1-\frac{X_0}{K}\right)-\frac{a_1X_0Y_0}{b_1+X_0}, \\ D_*^{\alpha}Y &= \frac{c_1X_0Y_0}{b_1+X_0}+c_2Y_0-mY_0-\frac{a_2(1-p)Y_0^2}{b_2+(1-p)Y_0}. \end{aligned} \tag{6}$$

By applying eq. (3) to eq. (6), we obtain

$$\begin{aligned} X_1(\tau) &= X_0 + I^{\alpha}X_0\left[r\left(1-\frac{X_0}{K}\right)-\frac{a_1Y_0}{b_1+X_0}\right], \\ Y_1(\tau) &= Y_0 + I^{\alpha}Y_0\left[\frac{c_1X_0Y_0}{b_1+X_0}+c_2Y_0-mY_0-\frac{a_2(1-p)Y_0^2}{b_2+(1-p)Y_0}\right]. \end{aligned} \tag{7}$$

Using eq. (4), eq. (7) become

$$\begin{aligned} X_1(\tau) &= X_0 + \frac{\tau^{\alpha}X_0}{\Gamma(1+\alpha)}\left[r\left(1-\frac{X_0}{K}\right)-\frac{a_1Y_0}{b_1+X_0}\right], \\ Y_1(\tau) &= Y_0 + \frac{\tau^{\alpha}Y_0}{\Gamma(1+\alpha)}\left[\frac{c_1X_0Y_0}{b_1+X_0}+c_2Y_0-mY_0\right. \\ &\quad \left.-\frac{a_2(1-p)Y_0^2}{b_2+(1-p)Y_0}\right]. \end{aligned} \tag{8}$$

Furthermore, let $\tau \in [h, 2h)$; thus, $\frac{\tau}{h} \in [1, 2)$. Using eq. (5), we derive

$$\begin{aligned} D_*^\alpha X &= rX_1\left(1-\frac{X_1}{K}\right)-\frac{a_1X_1Y_1}{b_1+X_1}, \\ D_*^\alpha Y &= \frac{c_1X_1Y_1}{b_1+X_1}+c_2Y_1-pY_1-\frac{a_2(1-p)Y_1^2}{b_2+(1-p)Y_1}. \end{aligned} \tag{9}$$

By applying eq. (3) to the system (9), we obtain

$$\begin{aligned} X_2(\tau) &= X_1+I^\alpha X_1\left[r\left(1-\frac{X_1}{K}\right)-\frac{a_1Y_1}{b_1+X_1}\right], \\ Y_2(\tau) &= Y_1+I^\alpha Y_1\left[\frac{c_1X_1Y_1}{b_1+X_1}+c_2Y_1-pY_1-\frac{a_2(1-p)Y_1^2}{b_2+(1-p)Y_1}\right]. \end{aligned} \tag{10}$$

Using eq. (4), eq. (10) transform into

$$\begin{aligned} X_2(\tau) &= X_1+\frac{(\tau-h)^\alpha X_1}{\Gamma(1+\alpha)}\left[r\left(1-\frac{X_1}{K}\right)-\frac{a_1Y_1}{b_1+X_1}\right], \\ Y_2(\tau) &= Y_1+\frac{(\tau-h)^\alpha Y_1}{\Gamma(1+\alpha)}\left[\frac{c_1X_1Y_1}{b_1+X_1}+c_2Y_1-pY_1\right. \\ &\quad\left.-\frac{a_2(1-p)Y_1^2}{b_2+(1-p)Y_1}\right]. \end{aligned} \tag{11}$$

Now, let $\tau \in [2h, 3h)$, $\frac{\tau}{h} \in [2, 3)$, and according to eq. (5), we get

$$\begin{aligned} D_*^\alpha X &= rX_2\left(1-\frac{X_2}{K}\right)-\frac{a_1X_2Y_2}{b_1+X_2}, \\ D_*^\alpha Y &= \frac{c_1X_2Y_2}{b_1+X_2}+c_2Y_2-mY_2-\frac{a_2(1-p)Y_2^2}{b_2+(1-p)Y_2}. \end{aligned} \tag{12}$$

Applying eq. (3) to the system (12) yields

$$\begin{aligned} X_3(\tau) &= X_2+I^\alpha X_2\left[r\left(1-\frac{X_2}{K}\right)-\frac{a_1Y_2}{b_1+X_2}\right], \\ Y_3(\tau) &= Y_2+I^\alpha Y_2\left[\frac{c_1X_2Y_2}{b_1+X_2}+c_2Y_2-mY_2-\frac{a_2(1-p)Y_2^2}{b_2+(1-p)Y_2}\right]. \end{aligned} \tag{13}$$

Utilizing eq. (4), eq. (13) transform into

$$\begin{aligned} X_3(\tau) &= X_2+\frac{(\tau-2h)^\alpha X_2}{\Gamma(1+\alpha)}\left[r\left(1-\frac{X_2}{K}\right)-\frac{a_1Y_2}{b_1+X_2}\right], \\ Y_3(\tau) &= Y_2+\frac{(\tau-2h)^\alpha Y_2}{\Gamma(1+\alpha)}\left[\frac{c_1X_2Y_2}{b_1+X_2}+c_2Y_2-mY_2\right. \\ &\quad\left.-\frac{a_2(1-p)Y_2^2}{b_2+(1-p)Y_2}\right]. \end{aligned} \tag{14}$$

By iterating the same process n-times, we arrive at the following system.

$$\begin{aligned} D_*^\alpha X &= rX_n\left(1-\frac{X_n}{K}\right)-\frac{a_1X_nY_n}{b_1+X_n}, \\ D_*^\alpha Y &= \frac{c_1X_nY_n}{b_1+X_n}+c_2Y_n-mY_n-\frac{a_2(1-p)Y_n^2}{b_2+(1-p)Y_n}, \end{aligned} \tag{15}$$

for $\tau \in [nh, (n+1)h)$, $\frac{\tau}{h} \in [n, n+1)$. According to eq. (4), the solutions are given by

$$\begin{aligned} X_{n+1}(\tau) &= X_n+I^\alpha X_n\left[r\left(1-\frac{X_n}{K}\right)-\frac{a_1Y_n}{b_1+X_n}\right], \\ Y_{n+1}(\tau) &= Y_n+I^\alpha Y_n\left[\frac{c_1X_n}{b_1+X_n}+c_2-m-\frac{a_2(1-p)Y_n^2}{b_2+(1-p)Y_n}\right]. \end{aligned} \tag{16}$$

Using eq. (3), system (16) become

$$\begin{aligned} X_{n+1}(\tau) &= X_n+\frac{(\tau-nh)^\alpha X_n}{\Gamma(1+\alpha)}\left[r\left(1-\frac{X_n}{K}\right)-\frac{a_1Y_n}{b_1+X_n}\right], \\ Y_{n+1}(\tau) &= Y_n+\frac{(\tau-nh)^\alpha Y_n}{\Gamma(1+\alpha)}\left[\frac{c_1X_n}{b_1+X_n}+c_2-m\right. \\ &\quad\left.-\frac{a_2(1-p)Y_n}{b_2+(1-p)Y_n}\right]. \end{aligned} \tag{17}$$

By taking τ to approach $(n+1)h$, eq. (17) gives

$$\begin{aligned} X_{n+1} &= X_n+\frac{h^\alpha X_n}{\Gamma(1+\alpha)}\left[r\left(1-\frac{X_n}{K}\right)-\frac{a_1Y_n}{b_1+X_n}\right] \\ &\equiv F_1(X_n, Y_n), \\ Y_{n+1} &= Y_n+\frac{h^\alpha Y_n}{\Gamma(1+\alpha)}\left[\frac{c_1X_n}{b_1+X_n}+c_2-m-\frac{a_2(1-p)Y_n}{b_2+(1-p)Y_n}\right] \\ &\equiv F_2(X_n, Y_n). \end{aligned} \tag{18}$$

If we set α equal to 1, our model simplifies to a basic type of approximation called forward Euler. This method is used for models with first-order derivatives. In the next sections, we determine equilibrium points and their local stabilities. We also ran numerical simulations to see impact of derivative-order.

3. Model analysis

Lemma 1. *[31] Consider a difference equation*

$$x_{n+1} = F(x_n), x \in \mathbb{R}^2. \tag{19}$$

A point $\bar{x} \in \mathbb{R}^2$ is considered an equilibrium point of system (18) if it satisfies $\bar{x} = F(\bar{x})$. Let $\lambda_i, i = 1, 2$ denote the eigenvalues of the Jacobian matrix at fixed point $\bar{x}$ of system (18). The stability characteristics of $\bar{x}$ can be classified as follows.

1. *locally asymptotically stable (sink) if $|\lambda_i| < 1, i = 1, 2$,*
2. *unstable (source) if $|\lambda_i| > 1, i = 1, 2$,*
3. *unstable (saddle) if $\lambda_1 > 1$ and $\lambda_2 < 1$, or $\lambda_1 < 1$ and $\lambda_2 > 1$,*
4. *non-hyperbolic if $|\lambda_1| = 1$ or $|\lambda_2| = 1$.*

Lemma 2. *[32] Consider $\bar{E} = (\bar{X}, \bar{Y})$ is an equilibrium point of system. For the quadratic equation $\lambda^2 - tr(J(\bar{E}))\lambda + det(J(\bar{E})) = 0$, the roots satisfy $|\lambda_i| < 1, \forall i = 1, 2$, if and only if the following three conditions are satisfied.*

1. *$1 + tr(J(\bar{E})) + det(J(\bar{E})) > 0$;*
2. *$1 - tr(J(\bar{E})) + det(J(\bar{E})) > 0$;*

3. $det(J(\bar{E})) < 1$;

There are four equilibrium points, those are:
1. The extinction point for both populations, denoted as $E_0 = (0,0)$, is a fixed point that always exists within the positive quadrant $\mathbb{R}^2_+$.
2. The prey extinction point, given by
$$E_1 = \left(0, \frac{b_2(m-c_2)}{(c_2-m-a_2)(1-p)}\right).$$
E_1 exists in $\mathbb{R}^2_+$ if $0 < c_2 - m < a_2$.
3. The predator extinction point, represented as $E_2 = (K, 0)$, which consistently exists in $\mathbb{R}^2_+$ since K is a positive value.
4. The coexistence point $E_3 = (X^*, Y^*)$ with
$$\begin{aligned} X^* &= \frac{\sqrt[3]{Q_2 \pm \sqrt{Q_2^2 + \frac{4}{27}Q_1^3}}}{\sqrt[3]{2}} - \frac{Q_1\sqrt[3]{2}}{3\sqrt[3]{Q_2 \pm \sqrt{Q_2^2 + \frac{4}{27}Q_1^3}}} - \frac{B}{3A}, \\ Y^* &= \frac{r}{a_1}\left(1 - \frac{X_3}{K}\right)(b_1 + X_3), \\ Q_1 &= \frac{3AC - B^2}{3A^2}, \\ Q_2 &= \frac{9ABC - 2B^3 - 27A^2D}{27A^3}, \\ A &= \frac{r}{a_1K}(1-p)(a_2 - c_1 - c_2 + m), \\ B &= \frac{r}{a_1}(1-p)\Big[(c_1 + c_2 - m - a_2) - \frac{b_1}{K}(c_1 + 2(c_2 - m \\ &\quad - a_2))\Big], \\ C &= (c_1 + c_2 - m)b_2 + \frac{rb_1}{a_1}(1-p)\Big[c_1 + (2 - b_1)(c_2 - m) \\ &\quad - 2a_2 + \frac{a_2b_1}{K}\Big], \\ D &= b_1\left[b_2(c_2 - m) + \frac{rb_1}{a_1}(1-p)(c_2 - m - a_2)\right], \end{aligned} \tag{20}$$
if $a_2 + m \neq c_1 + c_2$. The point E_3 in eq. (20) is derived using Cardano's formula [33] and exists in $\mathbb{R}^2_+$ under the following conditions.
(a) $Q_2^2 + \frac{4}{27}Q_1^3 \geq 0$, and
(b) $0 < X^* < K$.
If $a_2 + m = c_1 + c_2$, the values of X^* and Y^* are given as follows.
$$\begin{aligned} X^* &= \frac{-C \pm \sqrt{C^2 - 4BD}}{2B}, \\ Y^* &= \frac{r}{a_1}\left(1 - \frac{X^*}{K}\right)(b_1 + X^*), \end{aligned} \tag{21}$$
with
$$\begin{aligned} B &= \frac{c_1rb_1}{a_1K}(1-p), \\ C &= a_2b_2 + \frac{rb_1}{a_1}(1-p)\left(b_1(c_1 - a_2) - c_1 + \frac{a_2b_1}{K}\right), \\ D &= b_1\left[b_2(a_2 - c_1) - \frac{rc_1b_1}{a_1}(1-p)\right]. \end{aligned} \tag{22}$$
The coexistence point exists in $\mathbb{R}^2_+$ if
(a) $C^2 - 4BD \geq 0$, and
(b) $0 < X^* < K$.

For any equilibrium point of system (18), $\bar{E}$, linearization of system (18) around $\bar{E}$ yield the Jacobian matrix
$$J(\bar{E}) = \begin{bmatrix} \frac{\partial F_1}{\partial X} & \frac{\partial F_1}{\partial Y} \\ \frac{\partial F_2}{\partial X} & \frac{\partial F_2}{\partial Y} \end{bmatrix}_{\bar{E}}, \tag{23}$$
where
$$\begin{aligned} \frac{\partial F_1}{\partial X}(\bar{E}) &= 1 + \frac{h^\alpha}{\Gamma(1+\alpha)}\left[r\left(1 - \frac{2\bar{X}}{K}\right) - \frac{a_1b_1\bar{Y}}{(b_1+\bar{X})^2}\right], \\ \frac{\partial F_1}{\partial Y}(\bar{E}) &= \frac{h^\alpha}{\Gamma(1+\alpha)}\left[-\frac{a_1\bar{X}}{b_1+\bar{X}}\right], \\ \frac{\partial F_2}{\partial X}(\bar{E}) &= \frac{h^\alpha}{\Gamma(1+\alpha)}\left[\frac{c_1b_1\bar{Y}}{(b_1+\bar{X})^2}\right], \\ \frac{\partial F_2}{\partial Y}(\bar{E}) &= 1 + \frac{h^\alpha}{\Gamma(1+\alpha)}\Big[-\frac{2a_2b_2(1-p)\bar{Y} + a_2(1-p)^2\bar{Y}^2}{(b_2+(1-p)\bar{Y})^2} + c_2 \\ &\quad + \frac{c_1\bar{X}}{b_1+\bar{X}} - m\Big]. \end{aligned} \tag{24}$$
The eigenvalues of the Jacobian matrix (23) are utilized to assess the local stability characteristics of the equilibrium points of system (18). These findings are presented in Theorem 1.

Theorem 1. *The local stability of the equilibrium points of system (18) are as follows.*
1. *Suppose that*
$$h_0 = \sqrt[\alpha]{\frac{2\Gamma(1+\alpha)}{m - c_2}}. \tag{25}$$
$E_0(0,0)$ is
   (a) *source if $c_2 > m$ or $c_2 < m$ and $h > h_0$,*
   (b) *saddle if $c_2 < m$ and $h < h_0$,*
   (c) *non-hyperbolic if $c_2 = m$ or $c_2 < m$ and $h = h_0$.*
2. *Let*
$$h_{1a} = \sqrt[\alpha]{\frac{2\Gamma(1+\alpha)}{\frac{a_1b_2(c_2-m)}{b_1(a_2-(c_2-m))(1-p)} - r}}, \tag{26}$$
$$h_{1b} = \sqrt[\alpha]{\frac{2a_2\Gamma(1+\alpha)}{(c_2-m)(a_2-(c_2-m))}}. \tag{27}$$
Prey extinction point $E_1\left(0, \frac{b_2(m-c_2)}{(c_2-m-a_2)(1-p)}\right)$ is
   (a) *sink if $r < \frac{a_1b_2(m-c_2)}{b_1(c_2-m-a_2)(1-p)}$, $h < h_{1a}$, and $h < h_{1b}$;*
   (b) *saddle if $r < \frac{a_1b_2(m-c_2)}{b_1(c_2-m-a_2)(1-p)}$, $h < h_{1a}$, and $h > h_{1b}$; or $r > \frac{a_1b_2(m-c_2)}{b_1(c_2-m-a_2)(1-p)}$ or $r < \frac{a_1b_2(m-c_2)}{b_1(c_2-m-a_2)(1-p)}$ and $h > h_{1a}$, and $h < h_{1b}$;*

(c) *non-hyperbolic if* $r = \dfrac{a_1b_2(m-c_2)}{b_1(c_2-m-a_2)(1-p)}$ *or* $r < \frac{a_1b_2(m-c_2)}{b_1(c_2-m-a_2)(1-p)}$ *and* $h = h_{1a}$, *or* $h = h_{1b}$;

(d) *source if* $r > \dfrac{a_1b_2(m-c_2)}{b_1(c_2-m-a_2)(1-p)}$ *or* $r < \frac{a_1b_2(m-c_2)}{b_1(c_2-m-a_2)(1-p)}$ *and* $h > h_{1a}$, *and* $h > h_{1b}$.

3. $E_2(K,0)$ *is locally asymtotically stable if* $c_1 < \dfrac{(e-c_2)(b_1+K)}{K}$ *and saddle if* $c_1 > \dfrac{(e-c_2)(b_1+K)}{K}$.
   (a) *sink if* $h < h_{2a}$, $m > c_2 + \dfrac{c_1K}{b_1+K}$, *and* $h < h_{2b}$;
   (b) *saddle if* $h < h_{2a}$, $m > c_2 + \dfrac{c_1K}{b_1+K}$, *and* $h > h_{2b}$; *or if* $h < h_{2a}$ *and* $m < c_2 + \dfrac{c_1K}{b_1+K}$;
   (c) *non-hyperbolic if* $h = h_{2a}$, *or* $m > c_2 + \dfrac{c_1K}{b_1+K}$, *and* $h = h_{2b}$;
   (d) *source if* $h > h_{2a}$, $m > c_2 + \dfrac{c_1K}{b_1+K}$, *and* $h > h_{2b}$.
4. $E_3(X^*,Y^*)$ *is locally asymtotically stable if* h *satisfy all of the following conditions.*
   (a) $1 + tr(J(E_3)) + det(J(E_3)) > 0$,
   (b) $1 - tr(J(E_3)) + det(J(E_3)) > 0$,
   (c) $det(J(E_3)) - 1 < 0$,

   with $tr(J(E_3))$ *and* $det(J(E_3))$ *are the trace and determinant of characteristic equation of the Jacobian matrix (23) at* E_3, *respectively. All of the three conditions will be computed numerically due to the terms' complexity.*

Proof. 1. By substituting $E_0(0,0)$ into (23), we obtain

$$J(E_0) = \begin{bmatrix} 1 + \dfrac{h^\alpha r}{\Gamma(1+\alpha)} & 0 \\ 0 & 1 + \dfrac{h^\alpha}{\Gamma(1+\alpha)}(c_2-m) \end{bmatrix}.$$

Since $|\lambda_1| = 1 + \frac{h^\alpha r}{\Gamma(1+\alpha)} > 1$, E_0 is always unstable. Let

$$h_0 = \sqrt[\alpha]{\frac{2\Gamma(1+\alpha)}{m-c_2}}. \tag{28}$$

(a) If $c_2 > m$ or $c_2 < m$ and $h > h_0$, then $|\lambda_2| = |1 + \frac{h^\alpha}{\Gamma(1+\alpha)}(c_2-m)| > 1$. Based on Lemma 1, E_0 is source.
(b) If $c_2 < m$ and $h < h_0$, then $|\lambda_2| = |1 + \frac{h^\alpha}{\Gamma(1+\alpha)}(c_2 - m)| < 1$ and E_0 is saddle.
(c) If $c_2 = m$ or $c_2 < m$ and $h = h_0$, then $|\lambda_2| = |1 + \frac{h^\alpha}{\Gamma(1+\alpha)}(c_2-m)| = 1$ and E_0 is non-hyperbolic.

2. The Jacobian matrix for E_1 is

$$J(E_1) = \begin{bmatrix} J_1 & 0 \\ J_2 & J_3 \end{bmatrix},$$

$$J_1 = 1 + \frac{h^\alpha}{\Gamma(1+\alpha)}\left[r - \frac{a_1b_2(c_2-m)}{b_1(a_2-(c_2-m))(1-p)}\right],$$

$$J_2 = \frac{h^\alpha}{\Gamma(1+\alpha)}\left[\frac{c_1b_2(m-c_2)}{b_1(c_2-m-a_2)(1-p)}\right],$$

$$J_3 = 1 + \frac{h^\alpha}{\Gamma(1+\alpha)}\left[\frac{(c_2-m)(c_2-m-a_2)}{a_2}\right].$$

$J(E_1)$ has eigenvalues

$$\lambda_1 = 1 + \frac{h^\alpha}{\Gamma(1+\alpha)}\left[r + \frac{a_1b_2(m-c_2)}{b_1(c_2-m-a_2)(1-p)}\right],$$

$$\lambda_2 = |1 + \frac{h^\alpha}{\Gamma(1+\alpha)}\left[\frac{(c_2-m)(c_2-m-a_2)}{a_2}\right].$$

The existence E_1 requires that $0 < c_2 - m < a_2$. This condition implies that $(c_2-m)(c_2-m-a_2) < 0$. Suppose that

$$h_{1a} = \sqrt[\alpha]{\frac{2\Gamma(1+\alpha)}{\frac{a_1b_2(c_2-m)}{b_1(a_2-(c_2-m))(1-p)} - r}},$$

$$h_{1b} = \sqrt[\alpha]{\frac{2a_2\Gamma(1+\alpha)}{(c_2-m)(a_2-(c_2-m))}},$$

then we can write that

$$\lambda_1 = 1 - 2\left(\frac{h}{h_{1a}}\right)^\alpha, \tag{29}$$

$$\lambda_2 = 1 - 2\left(\frac{h}{h_{1b}}\right)^\alpha. \tag{30}$$

(a) If $r < \dfrac{a_1b_2(m-c_2)}{b_1(c_2-m-a_2)(1-p)}$, $h < h_{1a}$, and $h < h_{1b}$, then $|\lambda_1| < 1$ and $|\lambda_2| < 1$. Based on Lemma 1, E_1 is sink.
(b) If $r < \dfrac{a_1b_2(m-c_2)}{b_1(c_2-m-a_2)(1-p)}$, $h < h_{1a}$, and $h > h_{1b}$, then $|\lambda_1| < 1$ and $|\lambda_2| > 1$. Based on Lemma 1, E_1 is saddle.
(c) If $r > \dfrac{a_1b_2(m-c_2)}{b_1(c_2-m-a_2)(1-p)}$ or $r < \dfrac{a_1b_2(m-c_2)}{b_1(c_2-m-a_2)(1-p)}$ and $h > h_{1a}$, and $h < h_{1b}$, then $|\lambda_1| > 1$ and $|\lambda_2| < 1$. Based on Lemma 1, E_1 is saddle.
(d) If $r = \dfrac{a_1b_2(m-c_2)}{b_1(c_2-m-a_2)(1-p)}$ or $r < \dfrac{a_1b_2(m-c_2)}{b_1(c_2-m-a_2)(1-p)}$ and $h = h_{1a}$, or $h = h_{1b}$, then $|\lambda_1| = 1$ or $|\lambda_2| = 1$. Based on Lemma 1, E_1 is non-hyperbolic.
(e) If $r > \dfrac{a_1b_2(m-c_2)}{b_1(c_2-m-a_2)(1-p)}$ or $r < \dfrac{a_1b_2(m-c_2)}{b_1(c_2-m-a_2)(1-p)}$ and $h > h_{1a}$, and $h > h_{1b}$, then $|\lambda_1| > 1$ and $|\lambda_2| > 1$. Based on Lemma 1, E_1 is source.

3. The Jacobian matrix for E_2 is

$$J(E_2) = \begin{bmatrix} M_1 & M_2 \\ 0 & M_3 \end{bmatrix},$$

$$M_1 = 1 - \frac{rh^\alpha}{\Gamma(1+\alpha)},$$

$$M_2 = -\frac{h^\alpha}{\Gamma(1+\alpha)}\left[\frac{a_1K}{b_1+K}\right],$$

$$M_3 = 1 + \frac{h^\alpha}{\Gamma(1+\alpha)}\left[\frac{c_1K}{b_1+K} + (c_2-m)\right].$$

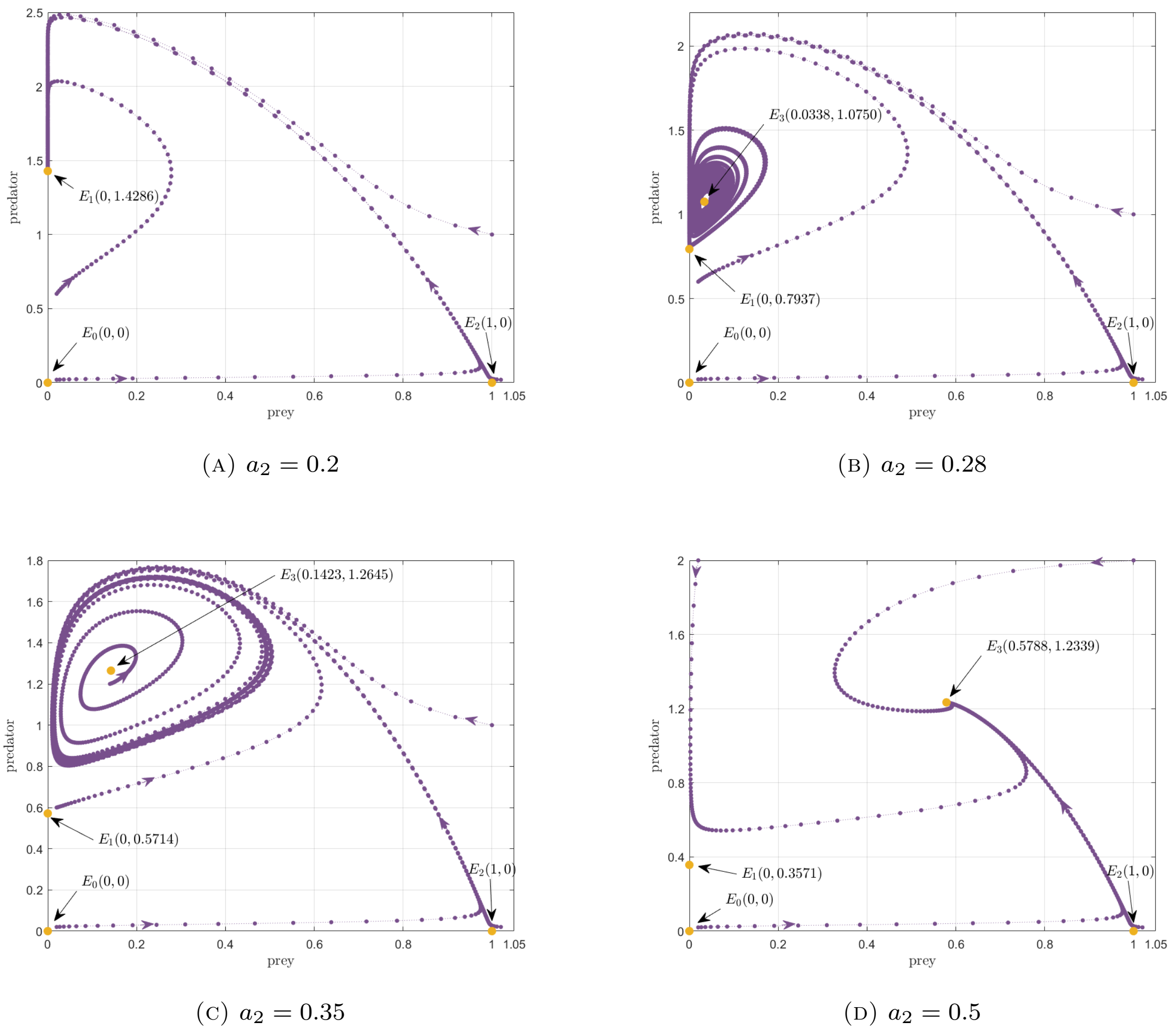

(A) $a_2 = 0.2$

(B) $a_2 = 0.28$

(C) $a_2 = 0.35$

(D) $a_2 = 0.5$

Figure 1. Simulation 1: Phase Portraits to Visualize the Effects of Predator Cannibalism

The eigenvalues are $1 - \frac{rh^\alpha}{\Gamma(1+\alpha)}$ and $\lambda_2 = 1 + \frac{h^\alpha}{\Gamma(1+\alpha)}\left[\frac{c_1 K}{b_1+K} + (c_2 - m)\right]$. Suppose that

$$h_{2a} = \sqrt[\alpha]{\frac{2\Gamma(1+\alpha)}{r}},$$
$$h_{2b} = \sqrt[\alpha]{\frac{2a_2\Gamma(1+\alpha)}{m - c_2 - \frac{c_1 K}{b_1+K}}},$$

then we can write that

$$\lambda_1 = 1 - 2\left(\frac{h}{h_{2a}}\right)^\alpha,$$
$$\lambda_2 = 1 - 2\left(\frac{h}{h_{2b}}\right)^\alpha. \tag{31}$$

(a) If $h < h_{2a}$, $m > c_2 + \dfrac{c_1 K}{b_1 + K}$, and $h < h_{2b}$, then $|\lambda_1| < 1$ and $|\lambda_2| < 1$. Based on Lemma 1, E_2 is sink.

(b) If $h < h_{2a}$, $m > c_2 + \dfrac{c_1 K}{b_1 + K}$, and $h > h_{2b}$, then $|\lambda_1| < 1$ and $|\lambda_2| > 1$. Based on Lemma 1, E_2 is saddle.

(c) If $h < h_{2a}$ and $m < c_2 + \dfrac{c_1 K}{b_1 + K}$, then $|\lambda_1| < 1$ and $|\lambda_2| > 1$. Based on Lemma 1, E_2 is saddle.

(d) If $h = h_{2a}$, or $m > c_2 + \dfrac{c_1 K}{b_1 + K}$, and $h = h_{2b}$, then $|\lambda_1| = 1$ or $|\lambda_2| = 1$. Based on Lemma 1, E_2 is non-hyperbolic.

(e) If $h > h_{2a}$, $m > c_2 + \dfrac{c_1 K}{b_1 + K}$, and $h > h_{2b}$, then $|\lambda_1| > 1$ and $|\lambda_2| > 1$. Based on Lemma 1, E_2 is source.

4. The Jacobian matrix for coexistence point is

$$J(E_3) = \begin{bmatrix} N_1 & N_2 \\ N_3 & N_4 \end{bmatrix},$$

where

$$N_1 = 1 + \frac{h^\alpha}{\Gamma(1+\alpha)}\left[r\left(1 - \frac{2X^*}{K}\right) - \frac{a_1 b_1 Y^*}{(b_1 + X^*)^2}\right],$$
$$N_2 = \frac{h^\alpha}{\Gamma(1+\alpha)}\left[-\frac{a_1 X^*}{b_1 + X^*}\right], \tag{32}$$

$$N_3 = \frac{h^\alpha}{\Gamma(1+\alpha)}\left[\frac{c_1 b_1 Y^*}{(b_1+X^*)^2}\right],$$
$$N_4 = 1 + \frac{h^\alpha}{\Gamma(1+\alpha)}\left[\frac{(c_2-m)(c_2-m-a_2)}{a_2}\right]. \quad (33)$$

The eigenvalues of $J(E_3)$ are the roots of the characteristic function

$$\lambda^2 - tr(J(E_3))\lambda + det(J(E_3)) = 0, \quad (34)$$

with $tr(J(E_3)) = J_{11} + J_{22}$ and $det(J(E_3)) = J_{11}J_{22} - J_{12}J_{21}$. According to Lemma 2, E_3 is locally asymtotically stable if all of the following three conditions are satisfied.

$$\begin{aligned} &(i) && 1 + tr(J(E_3)) + det(J(E_3)) > 0,\\ &(ii) && 1 - tr(J(E_3)) + det(J(E_3)) > 0,\\ &(iii) && det(J(E_3)) - 1 < 0. \end{aligned} \quad (35)$$

□

4. Simulation

Table 2. Parameters Value of Simulation 1 – 3

Parameter	Simulation 1	Simulation 2	Simulation 3
r	1	1	1
K	1	1	1
a_1	0.3	0.3	0.3
b_1	0.3	0.3	0.3
c_1	0.2	0.2	0.2
a_2	0.2/0.28/0.35/0.5	0.3	0.28
b_2	1	1	1
c_2	0.12	0.12	0.12
m	0.02	0.02	0.02
p	0.3	0.2/0.4/0.6	0.3
α	0.5	0.5	0.4/1

Table 3. Parameters Value of Simulation 4 – 6

Parameter	Simulation 4	Simulation 5	Simulation 6
r	1	1	1
K	1	1	1
a_1	0.3	0.5	0.3
b_1	0.3	0.3	0.3
c_1	0.2	0.1	0.2
a_2	0.2	0.3	0.3
b_2	1	1	1
c_2	0.12	0.2	0.12
m	0.02	0.3	0.02
p	0.3	0.3	0.4
α	0.5	0.5	0.5

In this section, we perform numerical simulations of the model (18) using Matlab software and PWCA method. Simulation 1, 2, and 3 allow us to observe the effects of cannibalism rate, proportion of predator refuge, and derivative order, α, on system behavior. Simulation 4, 5, and 6 aims to illustrate the dynamic analysis results concerning the stability of equilibrium points. In this simulation, different step sizes will be used to demonstrate the occurrence of period-doubling bifurcations numerically. Since there is no existing data related to our proposed model, the following numerical simulations are performed using hypothetical parameters in Table 2 and Table 3. Several pairs of parameter values are taken from [15].

In Simulation 1, a Caputo derivative order of $\alpha = 0.5$ and a stepsize of $h = 0.1$ were used. In Figure 1 (A), with cannibalism rate $a_2 = 0.2$, the system's equilibrium points are $E_0(0,0)$, $E_1(0,1.4286)$, and $E_2(1,0)$, while no coexistence point exists. Since the predator cannibalism rate is low, the primary food source for the predators remains the prey, causing the predator population to heavily rely on the prey population for survival. As a result, the system is driven toward the extinction of the prey at E_1, while the predator population also declines due to lack of food. Analytically, E_1 is local stable because its stability conditions, as outlined in Theorem 1, are satisfied, those are $r < \frac{a_1 b_2(m-c_2)}{b_1(c_2-m-a_2)(1-p)}$, $h < h_{1a} = 17.1019$, and $h < h_{1b} = 1256.6$. In Figure 1 (B), where $a_2 = 0.28$, we have the coexistence point $E_3(0.0338, 1.0750)$ exists but it is not asymptotically stable since the third condition of (35) is not satisfied, that is $det(J(E_3)) - 1 = 0.0016 > 0$. Predator self-regulation begins to reduce the pressure on the prey population. This shift allows both species to survive and oscillate around the coexistence point $E_3(0.0338, 1.0750)$. This differs from the result obtained by [15] without considering memory effects, where the solution converges to the coexistence point with these parameter values. Furthermore, increasing a_2 to 0.35 causes the solutions tend to a limit cycle around $E_3(0.1423, 1.2645)$ (see Figure 1 (C)). Finally, in Figure 1 (D), with $a_2 = 0.5$, the coexistence point $E_3(0.5788, 1.2339)$ becomes asymptotically stable since all of the conditions in (35) are satisfied.

Simulation 2 also utilizes Caputo derivative order of $\alpha = 0.5$ and stepsize of $h = 0.1$. When the refuge proportion of cannibalized predator is 0.2, the solutions tend to a limit cycle around the existence point $E_3(0.0890, 1.1813)$, while the other three equilibrium points are unstable (see Figure 2 (A)). Furthermore, Figure 2 (B) shows that when the refuge proportion increases to 0.4, both populations coexist and converge to constant values: 0.0274 for prey population density and 1.0613 for predator population density. In Figure 2 (C), the refuge proportion is 0.6. Due to the substantial refuge proportion, predator can survive from cannibalism. The significantly high predator population density causes prey extinction, leading to the solution converging to the prey extinction point $E_1(0, 1.2500)$. This is consistent with analytical results due to the fulfillment of these conditions: $r < \frac{a_1 b_2(m-c_2)}{b_1(c_2-m-a_2)(1-p)}$, $h < h_{1a} = 17.1019$, and $h < h_{1b} = 706.8583$.

Simulation 3 is conducted to demonstrate the impact of memory effects to the system. In Figure 3 (A), the memory effect is considered with the Caputo derivative order of $\alpha = 0.4$. The system gradually stabilizes into a limit cycle around the coexistence point $E_3(0.0338, 1.0750)$. In contrast, Figure 3 (B) shows that when the memory effect is absent ($\alpha = 1$), the solution directly settles at the coexistence point E_3. The emergence of a limit cycle suggests continuous fluctuations in population levels, indicating a recurring pattern in predator-prey interactions. Without the memory effect, however, the system stabilizes at a steady coexistence state. This comparison underscores the significance of memory in sustaining long-term population fluctuations.

Subsequently, Simulations 4 – 6 were conducted to confirm the analytical results of the local stability of the equilibrium points E_1, E_2, and E_3 as presented in Theorem 1. Figure 4 shows

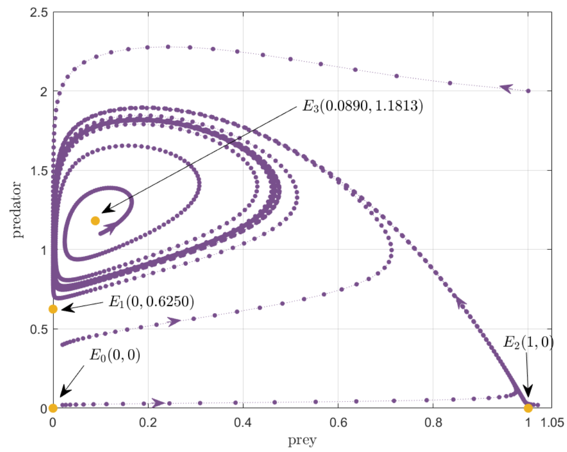

(A) $p = 0.2$

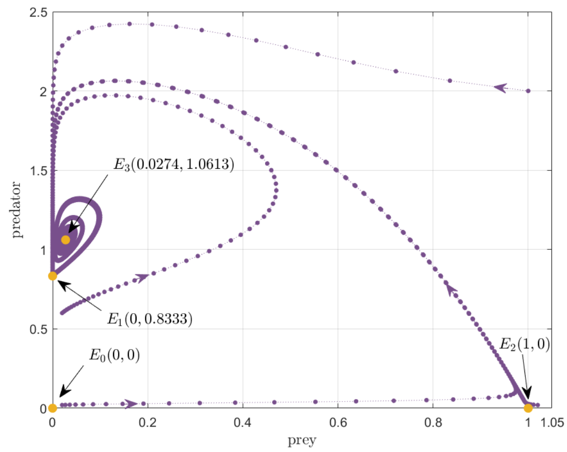

(B) $p = 0.4$

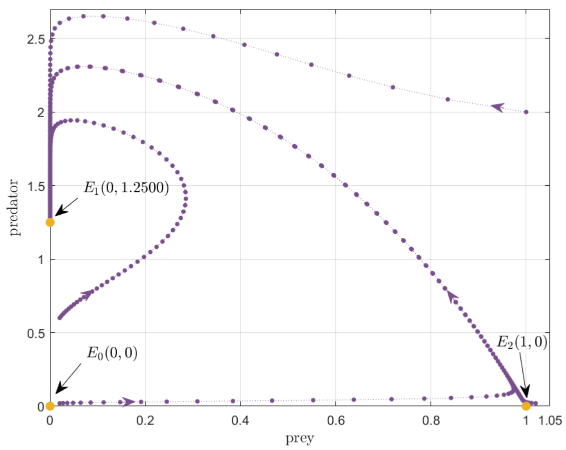

(C) $p = 0.6$

Figure 2. Simulation 2: Phase Portraits to Visualize the Effects of Predator Refuge

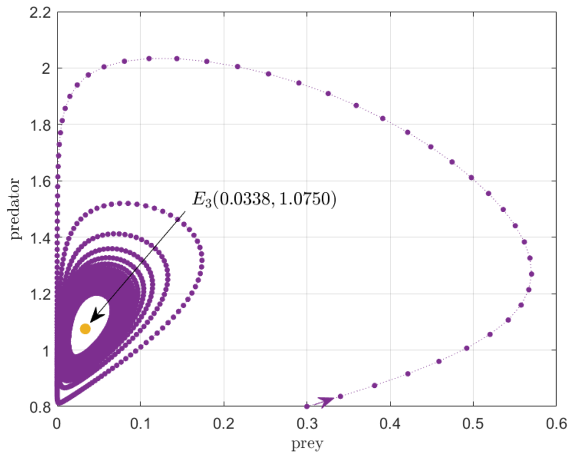

(A) $\alpha = 0.4$

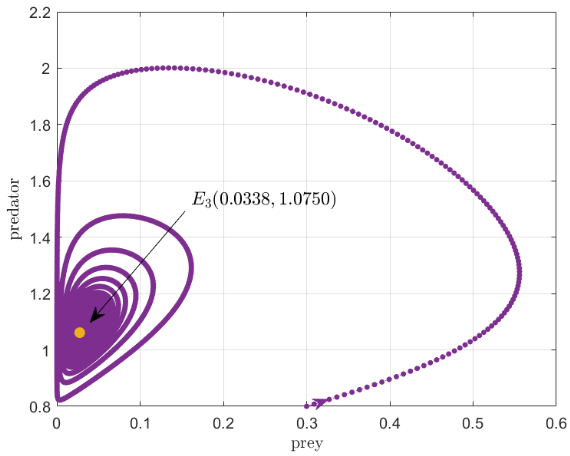

(B) $\alpha = 1$

Figure 3. Simulation 3: Phase Portraits to Visualize the Impacts of Memory Effect

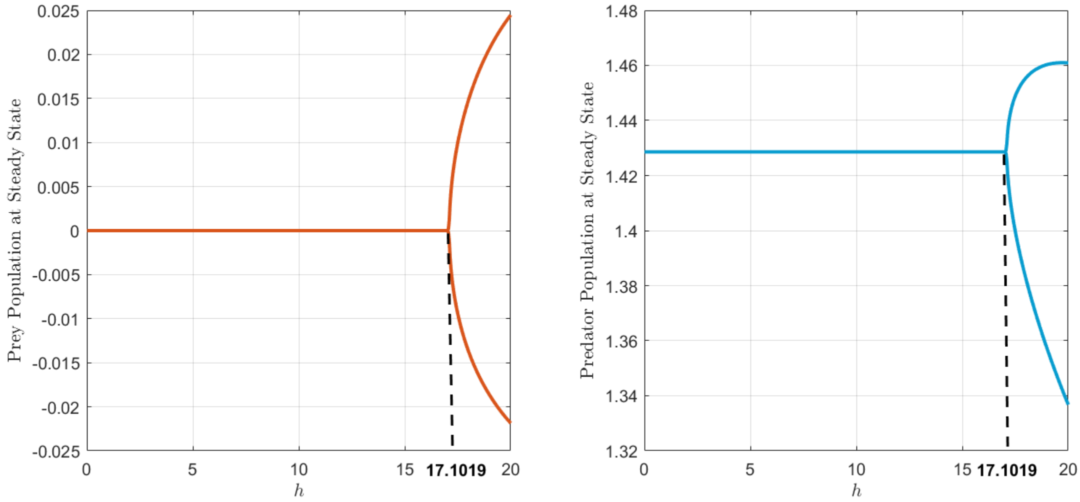

Figure 4. Simulation 4: The Stability of the Prey Extinction Point with Bifurcation Parameter h

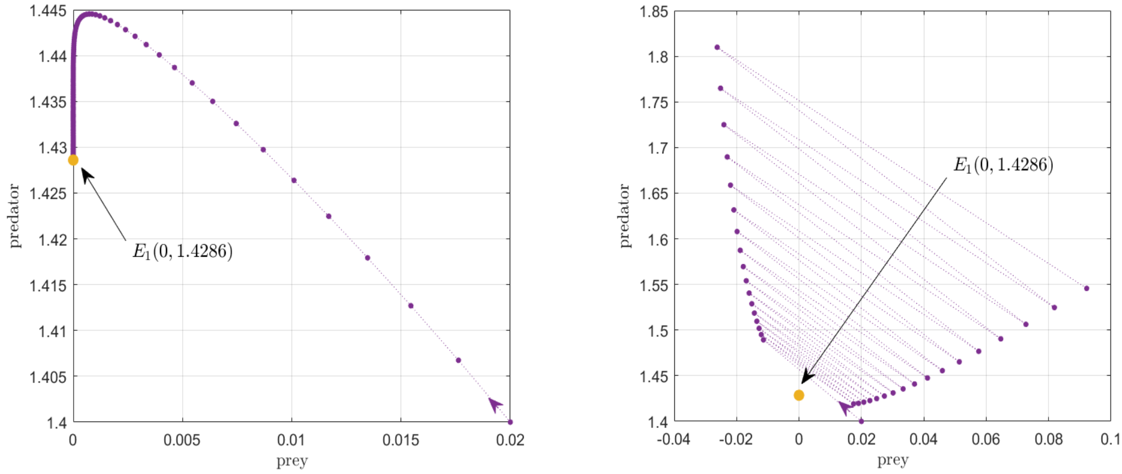

(A) $h = 0.1$ (B) $h = 17.5$

Figure 5. Simulation 4: Phase Portraits to Visualize The Stability of the Prey Extinction Point

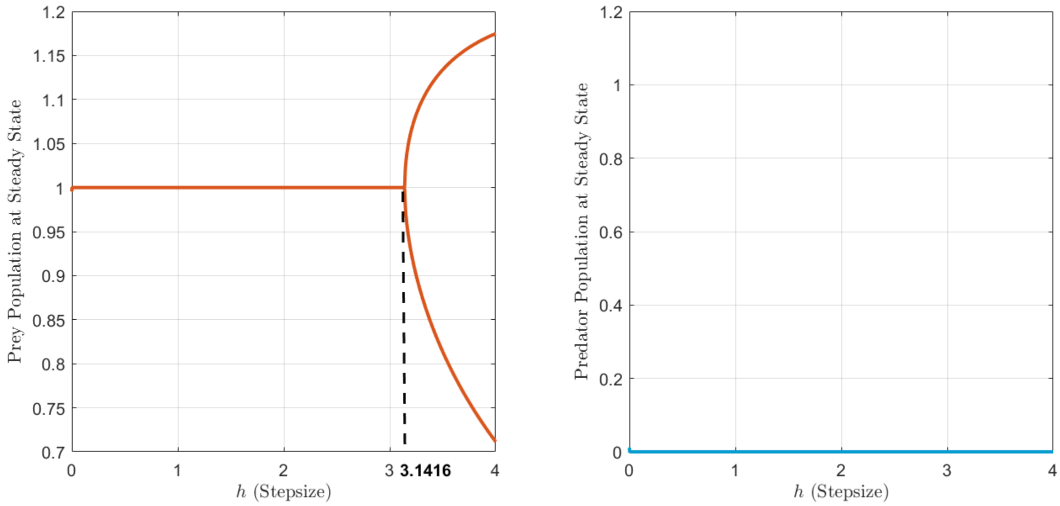

Figure 6. Simulation 5: The Stability of the Predator Extinction Point with Bifurcation Parameter h

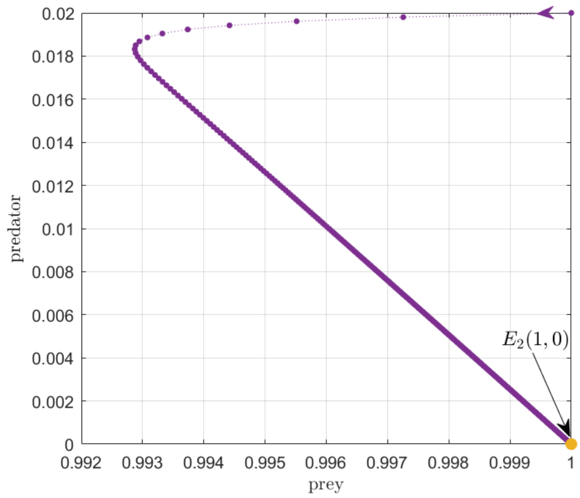

(A) $h = 0.1$

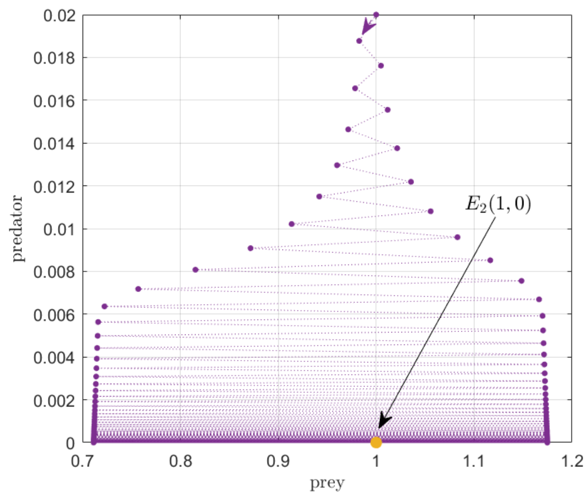

(B) $h = 4$

Figure 7. Simulation 5: Phase Portraits to Visualize The Stability of the Predator Extinction Point

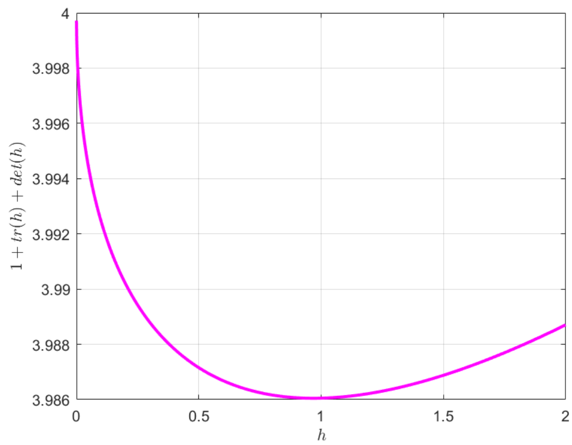

(A) $1 + tr(h) + det(h)$

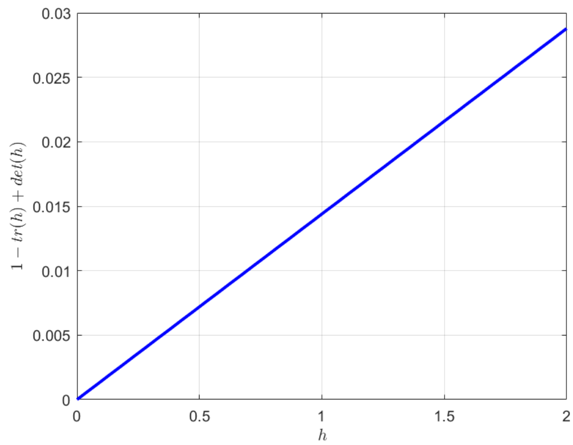

(B) $1 - tr(h) + det(h)$

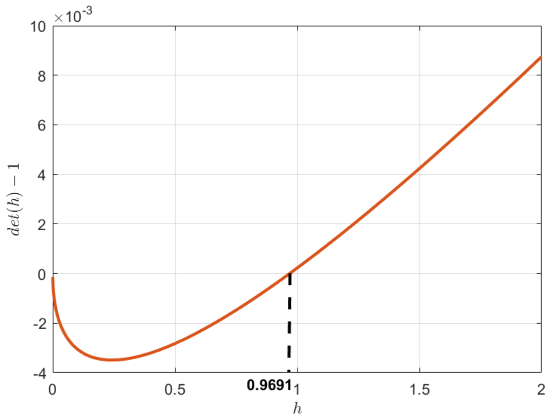

(C) $det(h) - 1$

Figure 8. Simulation 6: The Stability of The Coexistence Point with Bifurcation Parameter h

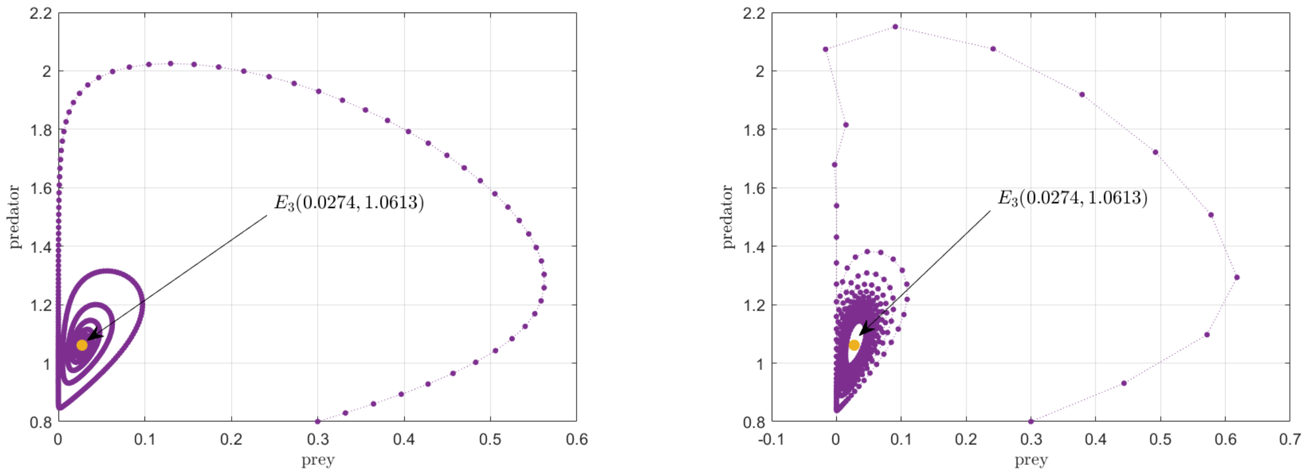

(A) $h = 0.1$ (B) $h = 2$

Figure 9. Simulation 6: Phase Portraits to Visualize The Stability of The Coexistence Point

how the step size (h) from Simulation 4 affects the stability of the prey extinction point. $h = \min\{h_{1a}, h_{1b}\} = 17.1019$ is the bifurcation point. A value of $h < 17.1019$ maintains the prey extinction point. However, it becomes unstable when h surpasses 17.1019. Phase portraits for two distinct values of h: 0.1 and 17.5 are provided in Figure 5 to illustrate this. The system settles at $E_1(0, 1.4286)$ at $h = 0.1$. However, at $h = 17.5$, the solution begins to oscillate and shifts away from E_1.

The stability shift also takes place at the predator extinction point for Simulation 5 parameter levels. The stability shift is shown to occur at $h = \min\{h_{2a}, h_{2b}\} = 3.1416$ in Figure 6. The extinction point of the predator is asymptotically stable for $h < 3.1416$. In contrast, it becomes unstable when $h > 3.1416$. Phase portraits are shown in Figure 7 for $h = 0.1$ and $h = 4$ to illustrate this phenomena. The solution approaches the equilibrium point $E_2(1, 0)$ with a step size of $h = 0.1$. At $h = 4$, on the other hand, the solution deviates from E_2 for the prey population density and displays oscillating behavior.

Like the extinction points for prey and predators, the coexistence point E_3 may likewise experience stability variations. Figure 8 shows the graphs of each condition as functions of h: $1 + tr(h) + det(h)$, $1 - tr(h) + det(h)$, and $det(h) - 1$. This shows the change in the fulfillment of the stability conditions for E_3. Any step size h satisfies the first two requirements ($1 + tr(h) + det(h) > 0$ and $1 - tr(h) + det(h) > 0$). Nevertheless, the third requirement ($det(h) - 1 < 0$) is only satisfied when $h < 0.9691$. The phase portraits for $h = 0.1$ and $h = 2$ are displayed in Figure 9 to illustrate this. When the step size is $h = 0.1$, the coexistence point E_3 is locally asymptotically stable, while the solution approaches a limit cycle around E_3 for $h = 2$.

5. Conclusion

In this study, we discretized a Caputo-type fractional-order predator-prey model involving predator cannibalism and refuge, using the Piecewise Constant Argument (PWCA) method. We then analyzed the dynamics of the resulting discrete system by determining the equilibrium points and their stability. Four equilibrium points were identified: the origin (where both populations are extinct), prey extinction, predator extinction, and coexistence. The stability properties of these equilibrium points were found to be more intricate compared to the continuous model. Specifically, the origin point was unstable, while the prey extinction, predator extinction, and coexistence points were conditionally locally asymptotically stable, depending on the parameter values. Furthermore, it was demonstrated that the stability of these equilibrium points was influenced by the order of the fractional derivative, which complicated the behavior of the system. The stability of the equilibrium points was also significantly influenced by the step size selection. These theoretical conclusions were validated by numerical simulations, which showed how adjustments to the model's parameters affect the dynamics of the system. With possible uses in biodiversity management and conservation, this work paves the way for additional investigation of fractional-order models in ecological and biological systems.

Author Contributions. **Rayungsari, M.**: Conceptualization, Methodology, Software, Formal analysis, Investigation, Resources, Data curation, Writing—original draft, Visualization, Funding Acquisition. **Nurmalitasari, D.**: Methodology, Formal analysis, Investigation, Writing—reviewing and editing, Visualization, Project administration. **Pamungkas, E. T. G. D.**: Methodology, Formal analysis, Investigation, Data curation, Writing—reviewing and editing, Visualization. All authors have read and agreed to the published version of the manuscript.

Acknowledgement. The authors express their gratitude to the Indonesian Ministry of Education, Culture, Research, and Technology (Kemdikbudristek) for funding this research and publication through the Beginner Lecturer Research Grant. The authors also sincerely appreciate the insightful comments and suggestions provided by the editor and anonymous reviewers, which have significantly contributed to improving the quality of this paper.

Funding. This research was funded by the Beginner Lecturer Research Grant from the Indonesian Ministry of Education, Culture, Research, and Technology (Kemdikbudristek), based on

Decree Number 0459/E5/PG.02.00/2024 dated May 30, 2024, and Agreement/Contract Number 109/E5/PG.02.00.PL/2024 dated June 11, 2024, 071/SP2H/PT/LL7/2024 dated June 12, 2024, and 2080.a\UNIWARA\LT\2024 dated June 12, 2024.

Conflict of interest. All authors report no conflict of interest relevant to this article.

Data availability. Not applicable.

References

[1] B. K. Das *et al.*, "Modeling predator–prey interaction: effects of perceived fear and toxicity on ecological communities," *International Journal of Dynamics and Control*, vol. 12, no. 7, pp. 2203–2235, 2024. DOI:10.1007/s40435-023-01343-x

[2] S. Bruers *et al.*, "Nature without suffering: Herbivorisation of predator species for the compassionate stewardship of earth's ecosystems," *Journal of Applied Animal Ethics Research*, vol. 6, no. 2, pp. 175–204, 2024. DOI:10.1163/25889567-bja10051

[3] K. Iamba and D. Dono, "A review on brown planthopper (nilaparvata lugens stål), a major pest of rice in asia and pacific," *Asian Journal of Research in Crop Science*, vol. 6, no. 4, pp. 7–19, 2021. DOI:10.9734/ajrcs/2021/v6i430122

[4] E. Surmaini *et al.*, "Climate change and the future distribution of brown planthopper in indonesia: A projection study," *Journal of the Saudi Society of Agricultural Sciences*, vol. 23, no. 2, pp. 130–141, 2024. DOI:10.1016/j.jssas.2023.10.002

[5] J. Liu *et al.*, "Herbivore-induced rice volatiles attract and affect the predation ability of the wolf spiders, pirata subpiraticus and pardosa pseudoannulata," *Insects*, vol. 13, no. 1, p. 90, 2022. DOI:10.3390/insects13010090

[6] P. S. Rupawate *et al.*, "Role of gut symbionts of insect pests: A novel target for insect-pest control," *Frontiers in Microbiology*, vol. 14, p. 1146390, 2023. DOI:10.3389/fmicb.2023.1146390

[7] L. K. Beay and M. Saija, "Dynamics of a stage–structure rosenzweig–macarthur model with linear harvesting in prey and cannibalism in predator," *Jambura Journal of Biomathematics (JJBM)*, vol. 2, no. 1, pp. 42–50, 2021. DOI:10.34312/jjbm.v2i1.10470

[8] D. Bhattacharjee *et al.*, "Stage structured prey-predator model incorporating mortal peril consequential to inefficiency and habitat complexity in juvenile hunting," *Heliyon*, vol. 8, no. 11, 2022. DOI:10.1016/j.heliyon.2022.e11365

[9] M. Rayungsari, R. R. Musafir, and D. Savitri, "Dynamics of a fractional-order predator-prey model incorporating allee effect and cannibalism," in *AIP Conference Proceedings*, vol. 3302, no. 1. AIP Publishing, 2025. DOI:10.1063/5.0261992

[10] R. K. Vijendravarma, "Diverse strategies that animals use to deter intraspecific predation," *Journal of Evolutionary Biology*, vol. 36, no. 7, pp. 967–974, 2023. DOI:10.1111/jeb.14129

[11] N. Hasan, A. Suryanto, and Trisilowati, "Dynamics of a fractional-order eco-epidemic model with allee effect and refuge on prey," *Commun. Math. Biol. Neurosci.*, vol. 2022, pp. Article–ID 117, 2022. DOI:10.28919/cmbn/7742

[12] P. Santra, H. S. Panigoro, and G. Mahapatra, "Complexity of a discrete-time predator-prey model involving prey refuge proportional to predator," *Jambura Journal of Mathematics*, vol. 4, no. 1, pp. 50–63, 2022. DOI:10.34312/jjom.v4i1.11918

[13] Sajan, Anshu, and, B. Dubey, "Study of a cannibalistic prey–predator model with allee effect in prey under the presence of diffusion," *Chaos, Solitons & Fractals*, vol. 182, p. 114797, 2024. DOI:10.1016/j.chaos.2024.114797

[14] J. A. Rosenheim and S. J. Schreiber, "Pathways to the density-dependent expression of cannibalism, and consequences for regulated population dynamics," *Ecology*, vol. 103, no. 10, p. e3785, 2022. DOI:10.1002/ecy.3785

[15] M. Rayungsari *et al.*, "Dynamical analysis of a predator-prey model incorporating predator cannibalism and refuge," *Axioms*, vol. 11, no. 3, p. 116, 2022. DOI:10.3390/axioms11030116

[16] M. Rayungsari *et al.*, "Dynamics analysis of a predator–prey fractional-order model incorporating predator cannibalism and refuge," *Frontiers in Applied Mathematics and Statistics*, vol. 9, p. 1122330, 2023. DOI:10.3389/fams.2023.1122330

[17] M. Rayungsari *et al.*, "A nonstandard numerical scheme for a predator-prey model involving predator cannibalism and refuge," *Communication in Biomathematical Sciences*, vol. 6, pp. 11–23, 2023. DOI:10.5614/cbms.2023.6.1.2

[18] H. S. Panigoro *et al.*, "Dynamics of an eco-epidemic predator–prey model involving fractional derivatives with power-law and mittag–leffler kernel," *Symmetry*, vol. 13, no. 5, p. 785, 2021. DOI:10.3390/sym13050785

[19] M. D. Johansyah *et al.*, "The existence and uniqueness of riccati fractional differential equation solution and its approximation applied to an economic growth model," *Mathematics*, vol. 10, no. 17, p. 3029, 2022. DOI:10.3390/math10173029

[20] H. S. Panigoro, M. Rayungsari, and A. Suryanto, "Bifurcation and chaos in a discrete-time fractional-order logistic model with allee effect and proportional harvesting," *International Journal of Dynamics and Control*, vol. 11, no. 4, pp. 1544–1558, 2023. DOI:10.1007/s40435-022-01101-5

[21] R. R. Musafir *et al.*, "Comparison of fractional-order monkeypox model with singular and non-singular kernels," *Jambura Journal of Biomathematics (JJBM)*, vol. 5, no. 1, pp. 1–9, 2024. DOI:10.37905/jjbm.v5i1.24920

[22] A. O. Yunus, M. O. Olayiwola, and A. M. Ajileye, "A fractional mathematical model for controlling and understanding transmission dynamics in computer virus management systems," *Jambura Journal of Biomathematics (JJBM)*, vol. 5, no. 2, pp. 116–131, 2024. DOI:10.37905/jjbm.v5i2.25956

[23] D. Lin *et al.*, "Experimental study of fractional-order rc circuit model using the caputo and caputo-fabrizio derivatives," *IEEE Transactions on Circuits and Systems I: Regular Papers*, vol. 68, no. 3, pp. 1034–1044, 2021. DOI:10.1109/TCSI.2020.3040556

[24] M. J. Uddin and C. N. Podder, "Fractional order prey–predator model incorporating immigration on prey: Complexity analysis and its control," *International Journal of Biomathematics*, vol. 17, no. 05, p. 2350051, 2024. DOI:10.1142/S1793524523500511

[25] P. Santra, "Fear effect in discrete prey-predator model incorporating square root functional response," *Jambura Journal of Biomathematics (JJBM)*, vol. 2, no. 2, pp. 51–57, 2021. DOI:10.34312/jjbm.v2i2.10444

[26] D. Mukherjee, "Complex dynamics in a discrete-time model of two competing prey with a shared predator," *Jambura Journal of Biomathematics (JJBM)*, vol. 5, no. 2, pp. 71–82, 2024. DOI:10.37905/jjbm.v5i2.27453

[27] A. M. A. El-Sayed and S. M. Salman, "On a discretization process of fractional-order riccati differential equation," *J. Fract. Calc. Appl*, vol. 4, no. 2, pp. 251–259, 2013.

[28] H. S. Panigoro *et al.*, "A discrete-time fractional-order rosenzweig-macarthur predator-prey model involving prey refuge," *Commun. Math. Biol. Neurosci.*, vol. 2021, pp. Article–ID 77, 2021. DOI:10.28919/cmbn/6586

[29] A. Suryanto, I. Darti, and E. Cahyono, "Bifurcation analysis and chaos control of a discrete-time fractional order predator-prey model with holling type ii functional response and harvesting," *CHAOS Theory and Applications*, vol. 7, no. 1, pp. 87–98, 2025. DOI:10.51537/chaos.1581247

[30] H. Deng *et al.*, "Dynamic behaviors of lotka–volterra predator–prey model incorporating predator cannibalism," *Advances in Difference Equations*, vol. 2019, pp. 1–17, 2019. DOI:10.1186/s13662-019-2289-8

[31] S. Elaydi, *An Introduction to Difference Equations*, 3rd ed. San Antonio, Texas: Springer, 2005. DOI:10.1007/0-387-27602-5

[32] A. Suryanto, "Stability analysis of the euler discretization for sir epidemic model," in *AIP Conference Proceedings*, vol. 1602, no. 1. American Institute of Physics, 2014, pp. 375–379. DOI:10.1063/1.4882514

[33] S. Ganti and S. Gopinathan, "A note on the solutions of cubic equations of state in low temperature region," *Journal of Molecular Liquids*, vol. 315, p. 113808, 2020. DOI:10.1016/j.molliq.2020.113808